

RESEARCH

Open Access



# Evaluation of energy consumption of LPWAN technologies

Husam Rajab<sup>1\*</sup> , Husam Al-Amaireh<sup>2</sup>, Taoufik Bouguera<sup>3</sup> and Tibor Cinkler<sup>1</sup>

\*Correspondence:  
husamrajab@tmit.bme.hu

<sup>1</sup> Department of Telecommunications and Media Informatics, Budapest University of Technology and Economics, Budapest, Hungary

<sup>2</sup> Department of Measurement and Information Systems, Budapest University of Technology and Economics, Budapest, Hungary

<sup>3</sup> University of Bretagne Loire, Polytech Nantes, IETR, 44300 Nantes, France

## Abstract

The majority of IoT implementations demand sensor nodes to run reliably for an extended time. Furthermore, the radio settings can endure a high data rate transmission while optimizing the energy-efficiency. The LoRa/LoRaWAN is one of the primary low-power wide area network (LPWAN) technologies that has highly enticed much concentration. The energy limits is a significant issue in wireless sensor networks since battery lifetime that supplies sensor nodes have a restricted amount of energy and neither expendable nor rechargeable in most cases. A common hypothesis is that the energy consumed by sensors in sleep mode is negligible. With this hypothesis, the usual approach is to consider subsets of nodes that reach all the iterative targets. These subsets also called coverage sets, are then put in the active mode, considering the others are in the low-power or sleep mode. In this paper, we address this question by proposing an energy consumption model based on LoRa and LoRaWAN, which optimizes the energy consumption of the sensor node for different tasks for a period of time. Our energy consumption model assumes the following, the processing unit is in on-state along the working sequence which enhances the MCU unit by constructing it in low-power modes through most of the activity cycle, a constant time duration, and the radio module sends a packet of data at a specified transmission power level. The proposed analytical approach permits considering the consumed power of every sensor node element where the numerical results show that the scenario in which the sensor node transfers data to the gateway then receives an acknowledgment RX2 without receiving RX1 consumes the most energy; furthermore, it can be used to analyze different LoRaWAN modes to determine the most desirable sensor node design to reach its energy autonomy where the numerical results detail the impact of scenario, spreading factor, and bandwidth on power consumption.

**Keywords:** Internet of Things (IoT), LPWAN, LoRa, LoRaWAN, Energy consumption, Performance evaluation

## 1 Introduction

The term Internet of Things (IoT), being an umbrella indication, covers a wide area of applications. The conversion from conventional wired infrastructure to wireless connection has enabled further devices, applications, and services to interact with each other. IoT assures the integration of smart objects, sensors, internet protocols, and wireless technologies, to distribute data and interact through specified protocols [1]. The

Internet of Things (IoT) will extend the reach of the internet from only computers and smartphones to encompass other aspects of our environment, i.e., home automation, digitized health, smart parking, smart farming, smart grids, industrial internet, process controlling, etc. [2]. IoT key characteristics involve the capability of smart objects to collect data comprehensively, send the required data in a secure mechanism, and create intelligent post-processing on the accumulated data [3]. The fast-growing electronics, RF technologies, networking, and the development in computational power have made internet-empowering technologies more affordable, and continue to do so. The employment of radio-frequency identification (RFID), quick response (QR) codes, and wireless technology are determined by their short-range and high-throughput. Furthermore, the cellular networks 2G, 3G, and 4G are long-ranged and have a high throughput, forming approaches to facilitate the interaction among humans, people to devices, and devices to devices [4]. Machine-type communications (MTC) is a model that empowers devices to transfer information autonomously and execute transactions without human interference. MTC technologies can connect devices to virtually everything within a single network. These devices merge in a smart grid, business, energy sector, and smart houses [5, 6]. Sensor nodes enable the IoT paradigm by the transformation of wireless connectivity in a natural and harsh environment. Thus, nodes that need to function among various technologies should feature large-scale network infrastructure with low power consumption. These restrictions promote the introduction of the low power wide area network (LPWAN). The LPWAN technologies presented in Fig. 1, show a radical communication that assures the long-range with low power consumption and low-cost deployment [7]. It is mainly intended for applications that expect few messages per day to be transmitted in a wide radio range. In that regard, SigFox, LoRaWAN, and NB-IoT are the most popular technologies [8]. Energy consumption represents an essential role in IoT, particularly for battery-powered devices installed in remote or unattainable areas where a lifetime of 10+ years is coveted. Each task of the consumed power needs to

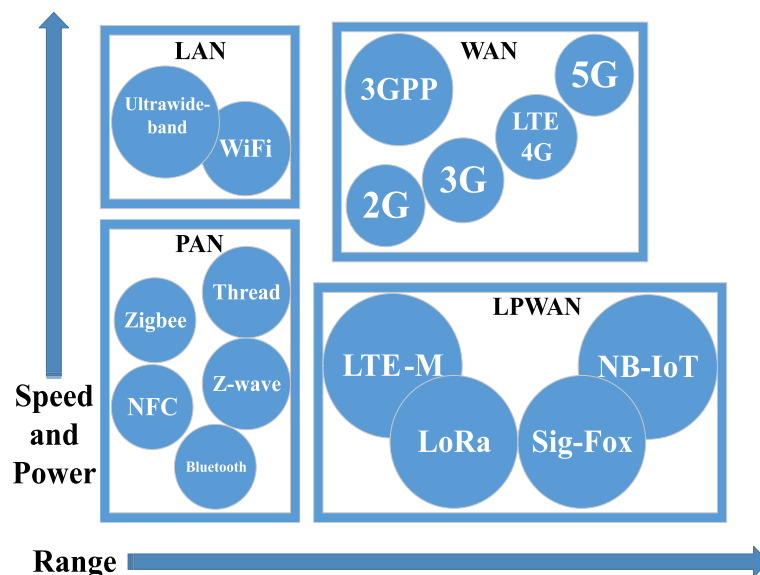


**Fig. 1** Low power wide area technologies

be carefully developed, and the design choices significantly influence the lifetime of the products. These design choices and trade-offs will be the subjects of investigation in this paper.

The proposed energy consumption model for sensor nodes using LoRa modulation and LoRaWAN protocol is estimated utilizing distinct LoRaWAN modes. The main purpose of this work is to focus on the energy efficiency of the LoRaWAN network that examines massive of concomitantly transmitting end-devices uniformly distributed around the gateway in a range of many kilometers. We investigate different scenarios, where in one case a sensor node transmits data to gateways considering outage probability caused by the imperfect channel behavior. Furthermore, we investigate the re-transmission of messages at certain times over the up-link radio channel which requires an acknowledgment from the gateway in one of two receive windows. Additionally, we develop a model and identify the properties that are related to the power consumption of LPWAN technologies to enable the developers to determine device lifetime and estimate the required battery energy capacities for systems. Moreover, we define the influence use cases have on consumption.

The paper proceeds as follows. “Related work” section presents related works. The background and the key characteristics of LoRa and LoRaWAN are presented in “LoRa and LoRaWAN overview” section. “Problem statements” section defined the problem statement. We investigate our proposed energy consumption mathematical analysis in “Methods/experimental” section, followed by the simulation and numerical results explained in “Analysis of the proposed scenarios” section. Finally, the conclusion and future works are presented in “Results and discussion” section.

## 2 Related work

LPWAN, LoRa, and LoRaWAN technologies overviews are provided in [9, 10]. In regards to the existing LPWAN technologies, LoRa has mainly attracted a wide variety of work because of the availability of commercial off-the-shelf radio transceivers and platforms [11–13]. Generally, LoRa operates with a bandwidth of 125 kHz; however, it also provides connections for bandwidths of 250 kHz and 500 kHz. The broader bands increase the resistance to fading, Doppler effects, channel noise, and long-term relative frequency for WAN devices [14]. The most recent research based on LoRa and LoRaWAN has focused on characteristics such as delay, range, throughput, and network capacity [15, 16]. Since the massive deployment of LoRa modulation for sensor applications, many papers investigated this new technology concerning its energy consumption. Certain studies have considered the ability of LoRa technology to determine the performance for various parameter settings in indoor [15, 17] or outdoor [9, 18, 19] configurations. Bor and Roedig introduce an algorithm for obtaining the most reliable transmission setting for a particular transmission channel in [15]. It operates a type of binary search of the parameter space, testing each setting for its packet response rate till a proper setup is found. The intention is to balance the cost of suitable finding parameters versus the packet delivery rate achieved. Cattani analyzed the optimal parameter settings in [20] by measuring the packet reception rate and energy efficiency for three types of channels (underground,

indoor, and outdoor) considering several LoRa parameter settings. The authors considered the effect of environmental parameters on channel performance and observed that high temperature at the node decreased the packet delivery rate considerably. The analytical model of LoRa energy consumption assigned to sleep, transmit, and receive conditions is proposed [21, 22]. The authors in [21] presented an optimization of the down-link communication in LoRaWAN while considering only a single SF, by deploying a battery lifetime of up to 1 year is achieved with 0.44 mJ energy consumption. On the other hand, the authors in [22] present an accurate calculation for message transmission time in LoRa. However, their study does not provide focus on the MAC layer mechanism, especially message acknowledgment, receive windows (RX1 and RX2), and re-transmissions. A short-range RF module CC1100 is used and presented in [23], which does not have the capabilities of LoRa technology. Furthermore, the authors explained the modeling of a sensor node aimed at wireless sensor network applications. A detailed explanation and illustration of LoRaWAN classes and their corresponding power consumption are discussed in [24]. A single gateway uplink model determining the path loss attenuation and Rayleigh fading is proposed in [25]. The authors utilized a stochastic geometry to model network interference and then disconnection and collision probabilities. Another energy estimation model is presented in [23]; the main object of this study is to obtain a low power consumption of sensor nodes. To conserve power, the authors have assumed that the communication module and the microcontroller must be in an idle state as much time as they are not active. Recently numerous investigations illustrated the power usage and current level of wireless sensor nodes in LoRaWAN networks without proposing an energy model to determine and enhance energy consumption and battery lifetime [26–28]. The authors in [29] proposed an energy consumption model for LoRaWAN devices. They determined the energy consumption for different devices, regardless of the network behavior. Determination data are obtained by employing the existing common LoRa hardware platform, Multi Connect mDot, based on the SX1272 transceiver. In contrast with [29], our proposed work estimates the energy cost and also evaluates the energy efficiency of LoRaWAN networks, considering the network with a massive number of end nodes. Our work contributes to measuring the energy cost of massive uniformly distributed end-devices in LoRaWAN. The energy model takes into consideration the transmission acknowledgment and its energy consumption cost, employing various LoRaWAN scenarios. The main goal of this research is to gain insight into competing LPWAN technologies, especially power consumption, which can assist IoT developers in making decisions when choosing internet-enabling technologies. In our paper, we have examined the performance of uplink communication and modeled different scenarios of the connected sensor. Moreover, we have demonstrated our energy model with optimization of LoRaWAN parameters for instance the spreading factor SF, the coding rate CR, the Bandwidth (BW), the payload size, and the communication range. Optimizing these parameters is essential to decrease the energy consumption of the sensor node. The average power consumption of a sensor node in different transmission modes serves to identify the operating lifetime. This research work contributes to measuring the energy cost of massive uniformly distributed end devices in

LoRaWAN. The energy model takes into consideration the transmission acknowledgment and its energy consumption cost, employing various LoRaWAN scenarios.

### 3 LoRa and LoRaWAN overview

This section gives a description of LoRa/LoRaWAN, covering essential characteristics and packet structures, and defining the procedure and critical parameters in transmitting information based on LoRa technology. LoRa, short for Long-Range, is a wireless communication modulation method, which employs a variety of Chirp Spreading Spectrum (CSS) to transmit information. The goal of this technology is to enhance the lifetime of battery-powered sensors with minimal cost. Long Range Wide Area Network, LoRaWAN, is the protocol, which is employed commonly with LoRa. The physical layer of LoRa is a closed and proprietary technology that is maintained by Semtech, while LoRaWAN is an open standard. The LoRaWAN protocol was developed by LoRa Alliance, which involves more than 500 member companies [30]. The network architecture is a star of stars type network as shown in Fig. 2.

LoRaWAN defines three categories of devices (Class A, B, and C) concerning the application usage, which results in having different power consumption profiles for each class. Figure 3 illustrates the distinctive classes which are defined as follows:

1. *Class A*: is expected to be the most commonly used class because it has the best power-saving capabilities [31]. End devices utilize the ALOHA protocol for scheduling up-link transmission in bi-directional communication. The end device sends a message at a random instance of time, and the gateway replies after two predefined delays. The messages in both receive windows are identical, which can cause colli-

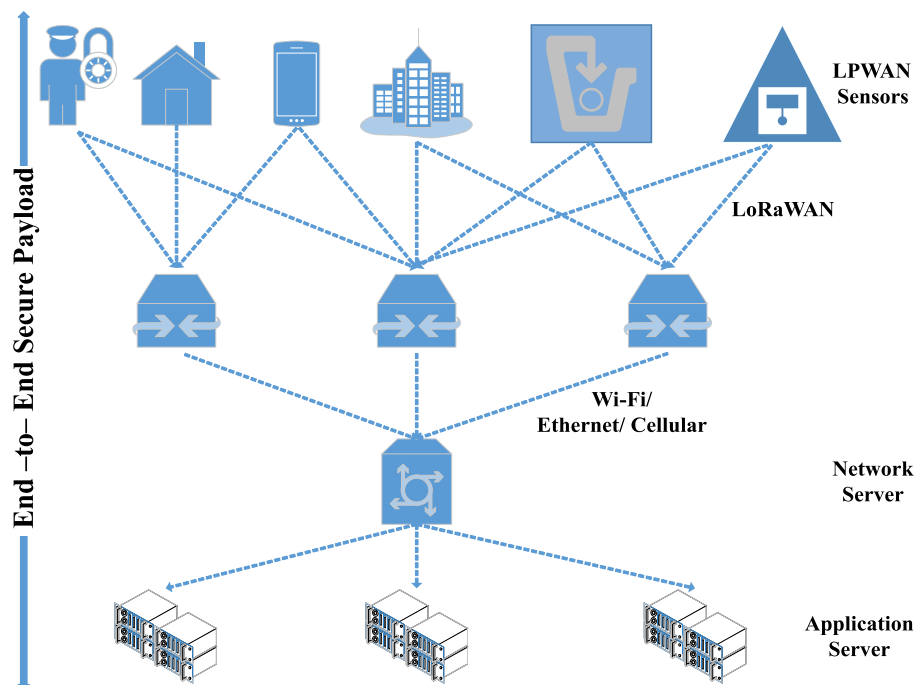
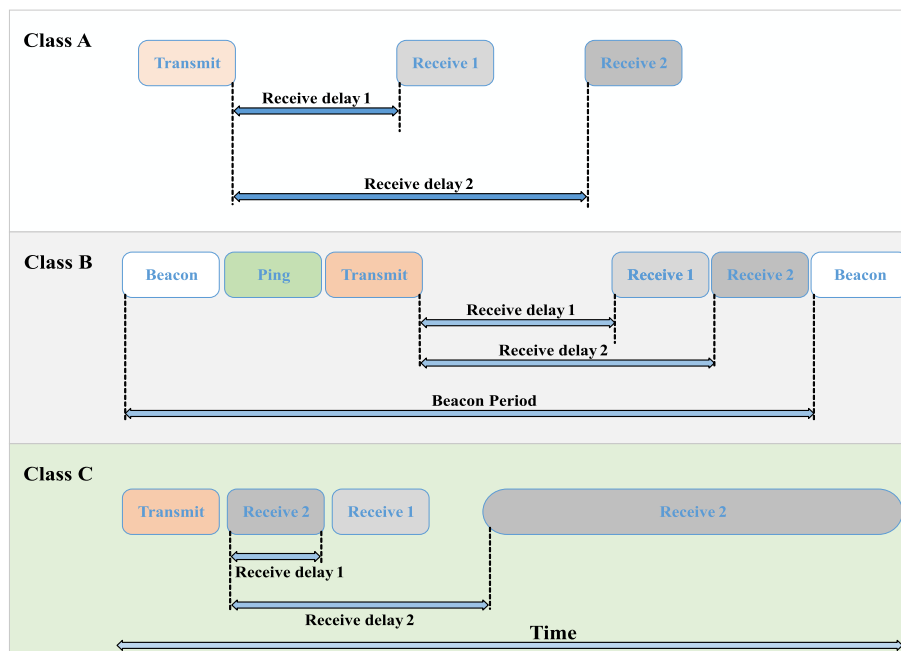


Fig. 2 LoRa network architecture



**Fig. 3** Device classes in LoRa

sion probability. Every node considers the acknowledgment in receive windows (RX1 and RX2) through downlink transmission. Time offset and data rate are fundamental parameters of receiving windows. Failure of acknowledgment in RX1 is the only reason for enabling the RX2. The default value for RX1 delay is one second, and two seconds for RX2 Delay.

2. *Class B*: allows devices to periodically receive slots and opens extra receiving slots at scheduled times. It enables the device to receive like class A devices, a ping slot generated by the gateway to combine end devices to receive additional windows. Therefore, a periodic beacon from the gateway for synchronization is required. The network server (NS) is informed of the listening status of end devices. The power consumption of Class B is higher than Class A [32, 33].
3. *Class C*: Devices always listen to the gateway, and it implements a traditional bi-directional communication system. End nodes consume the most energy since it represents the response of continuous listening of channel except while the transmission period [34].

The endless variation of frequency over time to encode data drives CSS modulation resistance versus the Doppler effect. However, the frequency offset connecting the transmitter and receiver reaches 20% of the total bandwidth without affecting the decoding performance. Accordingly, the crystal installed in transmitters is not expected to have maximum efficiency, which decreases the manufacturing cost of the LoRa transmitter. The following are several fundamental configuration parameters of LoRa radio:

- *Spreading factor (SF)*: is defined as the number of chirps per symbol. Also, it is a critical variable in LoRa, which has a significant influence on both the range, trans-

mission speed, and power consumption. LoRa has six different values in the range 7 to 12 to control the data rate of the transmitted signals [35]. Higher SF provides more extensive coverage areas; however, as a drawback, they increase the time-on-air (ToA) of LoRa packets and therefore the power consumption as well. The signals sent using different SFs are mutually quasi-orthogonal, meaning that messages can be transmitted concurrently without causing a collision. The symbol period,  $T_s$ , is given by:

$$T_s = \frac{2^{\text{SF}}}{\text{BW}} \quad (1)$$

So, the symbol rate,  $R_s$ , is the reciprocal of the symbol period:

$$R_s = \frac{\text{BW}}{2^{\text{SF}}} \quad (2)$$

The chip rate,  $R_c$ , which is the number of pulses per second, can be calculated as:

$$R_c = R_s \times 2^{\text{SF}} = \frac{\text{BW}}{2^{\text{SF}}} \times 2^{\text{SF}} = \text{BW} \quad (3)$$

The modulation rate or bit rate,  $R_b$ , is:

$$R_b = \text{SF} \times \frac{\text{BW}}{2^{\text{SF}}} \quad (4)$$

- *Carrier frequency (CF)*: Carrier Frequency (CF): It is the frequency employed to broadcast the information from node to gateway. LoRa operates at unlicensed frequency ISM bands in Europe and the U.S. at 865–870 MHz and 915 MHz, respectively [20, 36].
- *Bandwidth (BW)*: There are three bandwidth options for LoRa communication, i.e., 125 kHz, 250 kHz, and 500 kHz. In Europe, the 125 kHz is usually used for the 863–870 MHz frequency band. For fast transmission, it is more beneficial to use 500 kHz bandwidth, and if an extended coverage area is required, 125 kHz is recommended. Table 1 shows the relationship between BW, SF, and Receiver Sensitivity. An increase in bandwidth will lower the decoder sensitivity. Moreover, SF has a proportional relationship with receiver sensitivity.
- *Coding rate (CR)*: Coding rate expression is  $\text{CR} = \frac{4}{4+n}$  where  $n \in [1,2,3,4]$ . Minimizing the value of the code rate provides higher time-on-air (ToA) to transfer information. LoRa uses forward error correction. Whereas LoRa modulation is proprietary, reverse engineering endeavors determine that LoRa employs Hamming codes [37, 38], that

**Table 1** Semtech SX1276, sensitivity of LoRa receiver (dBm) [9]

BW (kHz)	SF7	SF8	SF9	SF10	SF11	SF12
125	– 126.50	– 127.25	– 131.25	– 132.75	– 134.50	– 133.25
250	– 124.25	– 126.75	– 128.25	– 130.25	– 132.75	– 132.25
500	– 120.75	– 124.00	– 127.50	– 128.75	– 128.75	– 133.25

increases the overhead of the transmitted messages and the nominal bit rate as the following:

$$R_b = SF \times \frac{BW}{2^{SF}} \times CR \quad (5)$$

The Hamming codes attach error detection and correction capabilities to the code. By increasing  $n$  by one, the code distance increases by one, which presents the capabilities specified in Table 2 [39]. The reduction in code rate leads to a decrease in the Packet Error Rate (PER) as opposed to the interference. For instance, an information message sent with a 4/8 code rate is more flexible to channel implications compared to a code rate of 4/5. As shown in Table 2 the lowest coding rate compares to a parity check bit, which can detect all uneven number of bit failures. The maximum that can be detected is 3-bit errors and it can correct 1-bit error.

*Transmission:* The LoRa sent messages including a preamble and payload:

$$T_{\text{packet}} = t_{\text{preamble}} + t_{\text{payload}} \quad (6)$$

The payload size can be varied by enabling or disabling portions of the payload together with adjusting the spreading factor, and coding rate. The number of payload symbols can be modeled as [40]:

$$n_{\text{payload}} = 8 + \max \left( \text{ceil} \left( \frac{[8\text{PL} - 4\text{SF} + 28 + 16\text{CRC} - 20\text{H}]}{4(\text{SF} - 2\text{DE})} \right) (\text{CR} + 4), 0 \right) \quad (7)$$

where:

- PL: Number of Payload bytes.
- SF: Spreading Factor 7–12.
- H: Header: 0 = enabled, 1 = no header.
- DE: Low Data Rate Optimization: 1 = enabled, 0 = disabled.
- CR: Coding rate.
- CRC: Cyclic Redundancy Check.

PL is the payload including both settings and the message payload as:

$$\text{PL} = \text{PL}_{\text{settings}} + \text{PL}_{\text{useful}} \quad (8)$$

**Table 2** Achievable error detection and correction capabilities in LoRa

Code rate	Error detection [Bits]	Error correction [Bits]
4/5	Parity	0
4/6	1	0
4/7	2	1
4/8	3	1

The number of preamble symbols can be modeled as:

$$n_{\text{preamble}} = 4.25 + n_{\text{regional}} \quad (9)$$

where  $n_{\text{regional}}$  is a regional constant, which is 8 in Europe.

By using the symbol duration the packet time on air can finally be represented as:

$$t_{\text{packet}} = (n_{\text{preamble}} + n_{\text{payload}}) \times t_{\text{symbol}} \quad (10)$$

Finally, multiplying the packet duration  $t_{\text{packet}}$  with the transmission power consumption  $P_{\text{TX}}$ , the energy consumption per transmission  $E_{\text{packet}}$  can be determined as shown below:

$$E_{\text{packet}} = t_{\text{packet}} \times P_{\text{TX}} \quad (11)$$

*Duty cycle:* European frequency bands are 867–869 MHz its duty cycle is 1%. It takes the time consumption  $t_{\text{packet}}$  for a node to send a group of data using this frequency band, so the current sending cycle of this node is  $T_C$ . The node can send data again after the end of the cycle, which can be determined as  $T_C - T_{TC}$ . So, the number of data transfers per day  $N_{\text{msg}}$  can be written as the following:

$$N_{\text{msg}} = \frac{24}{T_C - t_{\text{packet}}} \quad (12)$$

#### 4 Problem statements

LPWAN technologies must cope with the massive number of end nodes transmitting low data volume. Several methods have been considered recently, which help in the resolution of energy consumption and scalability problems. The design preferences, as mentioned in “LoRa and LoRaWAN overview” section, heavily influence device battery lifetimes. Designing a low-power consumption device within IoT requires multidisciplinary abilities within hardware, software, and RF. Also, the use cases need to be taken into concern when designing devices, as they are tightly connected with consumption. That brings the questions that our paper aims to answer:

- How can the power consumption of LPWAN devices be minimized?
- How do different use cases affect the power consumption of LPWAN devices?

#### 5 Methods/experimental

Considering the linear behavior of a battery in ideal scenarios, in a real-life scenario, battery characteristics degrade over time. Hence, these findings will only provide the approximation of the real node lifetime. Practically, there are three significant application places where battery-less devices will benefit: (i) Inaccessible or embedded devices, (ii) Enormous expansion of IoT networks (iii) Neglected devices after long-lifetime deployment. To demonstrate the application of our energy model, the assumed use case is relevant for fine-grained environmental monitoring. For instance: monitoring the air quality, occupancy in buildings or cities, or tracking goods in immense logistics warehouses.

### 5.1 Sensor node design

The sensor node is usually a micro-embedded system; its processing capacity, storage capacity, and communication capacity are limited. For better performance, the nodes need closer cooperation of hardware and software systems. The proposed node model is shown in Fig. 4, and the sensor nodes can use the access point of the LoRa/LoRaWAN radio module. The three main units of the sensor are a perception unit, a processing unit, and a communication unit.

- *Perception unit*: is composed of a sensor unit and an Analog to Digital Converter (ADC). The sensing unit is mainly used to collect all kinds of information in the real world, such as temperature, humidity, pressure, sound, and other physical details. Afterward, convert the analog information collected by the sensor into digital data, which is handed to the processing unit for processing.
- *Processing unit*: is composed of the central processing unit (CPU) and the memory. The processing unit is responsible for the data processing and operation of the whole sensor node, storing the collected data of this node and the data sent by other nodes. Our study in this paper uses an embedded system that is based on the STM32L073 microcontroller from ST Microelectronics [1] because these microcontrollers can be optimized for very low power consumption.
- *Communication unit*: is responsible for wireless communication with other sensor nodes, exchanging control messages, transmitting, and receiving data. Our model is based on LoRa/LoRaWAN Semtech Sx1272 transceiver. The current usage in each state and supply voltage is taken from the datasheet of the SX1272 in [40].

### 5.2 Energy model

The energy consumption of IoT sensor nodes can be illustrated by classifying the phases that the product operates in and after that the power consumed in each stage, as proposed in several publications on sensor networks [41, 42]. The model implies a constant duration and consumption. When the energy consumption in one message procedure is classified, the dissemination of power dissipation relying on the phases can be defined as well as the

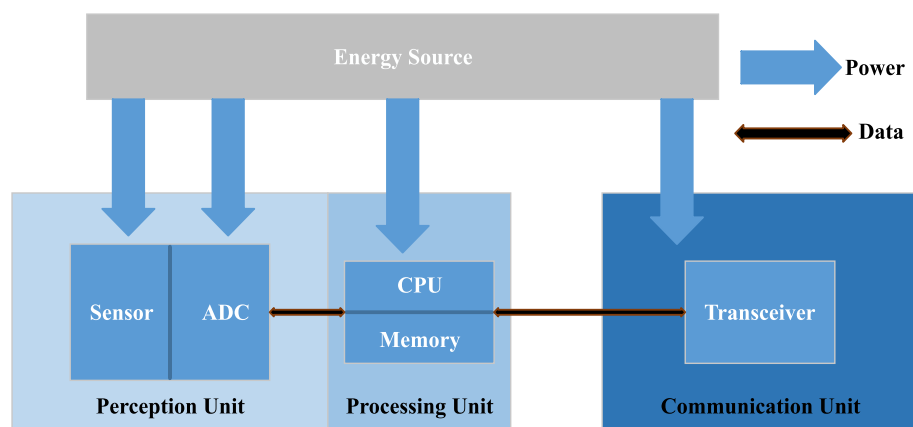


**Fig. 4** Sensor node

product battery lifetime. Figure 5 shows a division to multiple phases of operation of a typical IoT sensor node. The total consumed energy  $E_{TOTAL}$  used by the two main periods is given by the equation:

$$E_{TOTAL} = E_{Active} + E_{Sleep} \tag{13}$$

where  $E_{Active}$  is the energy consumed when the system is active and  $E_{Sleep}$  energy consumed when the system is in sleep mode.

Our energy consumption model concerning the following assumptions:

- As considered in [41, 43], the processing unit is in on-state along the working sequence. The presumption can enhance optimizing the MCU unit by constructing it in low-power modes through most of the activity cycle.
- A constant time duration characterizes each step of the sensor working sequence.
- The radio module sends a packet of data at a specified transmission power level.

The energy consumed in sleep mode is calculated as:

$$E_{Sleep} = P_{Sleep} \times t_{Sleep} \tag{14}$$

where  $P_{Sleep}$  and  $t_{Sleep}$  are the power consumption and duration in sleep mode, respectively.

The energy consumed in active mode can be determined as:

$$E_{Active} = E_{WU} + E_m + E_{proc} + E_{WUT} + E_{Tx} + E_{Rx} + E_{SP} \tag{15}$$

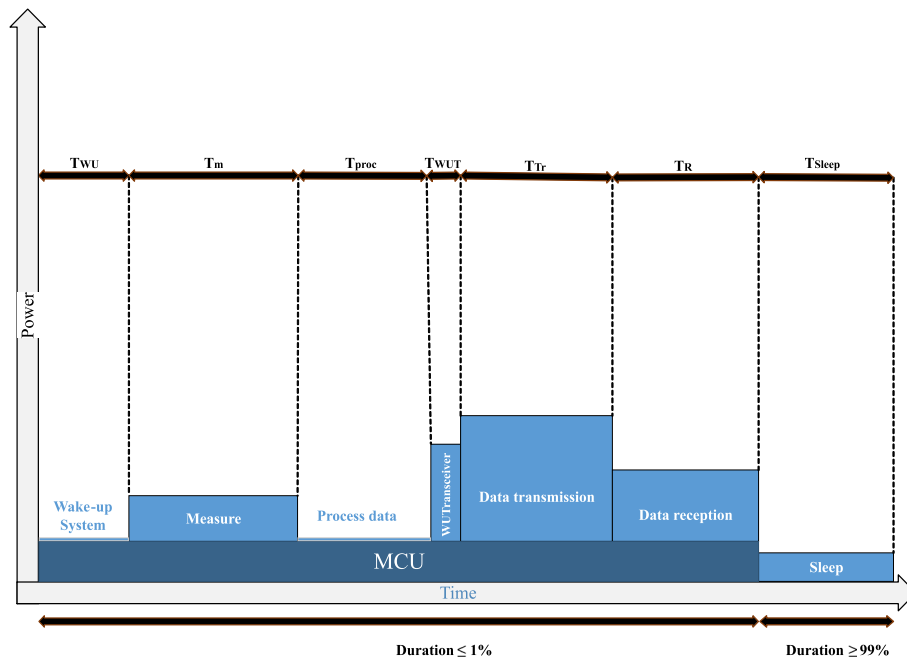


**Fig. 5** General state-based energy consumption model

where Fig. 5 illustrates the energies from each state. The energies are determined the same way as the energy in sleep mode by multiplying their power consumption with their duration.

### 5.3 Lifetime estimation

Presented with the transaction period and consumption of the node devices [41], the output lifetime can be estimated. To determine the lifetime LT of the devices, the battery capacity  $E_{\text{Bat}}$  can be divided by the energy consumption per day  $E_{\text{day}}$  as follows:

$$LT = \frac{E_{\text{Bat}}}{E_{\text{Day}}} \quad (16)$$

Equations 16, 17, and 18 The energy consumption essentially relies on the number of transactions  $n_{\text{msg}}$ , which defines the number of times the system is in an active state. The daily energy consumption can be determined as:

$$E_{\text{day}} = n_{\text{Msg}} \times E_{\text{Active}} + E_{\text{Sleep}} \quad (17)$$

$$n_{\text{msg}} = n_{\text{TX}} + n_{\text{RX}} \quad (18)$$

Considering that each transaction is bidirectional shown in (18). However, this is usually not the case in LPWAN as they often have more up-links than down-links. Taking this into account, the energy consumption per day  $E_{\text{day}}$  is given by:

$$E_{\text{day}} = n_{\text{TX}}(E_{\text{Active}} - E_{\text{RX}}) + n_{\text{RX}}(E_{\text{Active}} - E_{\text{TX}}) + E_{\text{Sleep}} \quad (19)$$

## 6 Analysis of the proposed scenarios

In this section, we will estimate and simulate the performance of our energy consumption model using a Class-A dense LoRaWAN network consisting of a single gateway and various end nodes. The presented range is sufficient for our application, and this enables saving the use of the battery. The uplink transmission of the end nodes is based on the ALOHA protocol. Furthermore, scenarios are proposed for the sensor node battery usage acceleration and transmission therefore the modules send data every 30 s.

This leaves the device with three possible message transaction scenarios illustrated in Fig. 6 as follows:

- *Scenario 1:* An unacknowledged transmission, where both receive windows are ignored.
- *Scenario 2:* An acknowledged transmission, where only one receive window is decoded Rx2.
- *Scenario 3:* An acknowledged transmission, where only one receive window is decoded Rx1.

The sensor node implements acceleration measurement and sends the acceleration value every 30 s. The operating frequency considered for the microcontroller is equal to 4

**Table 3** Characteristics of sensor node tasks [41]

Task	Time duration (ms)	Consumed power (mW)
Sensor (BMA220)	25	10.5
Data transmission (SX1272)	6.5	92.4
MCU STM32L073 (4 MHz)	33.5	1.8

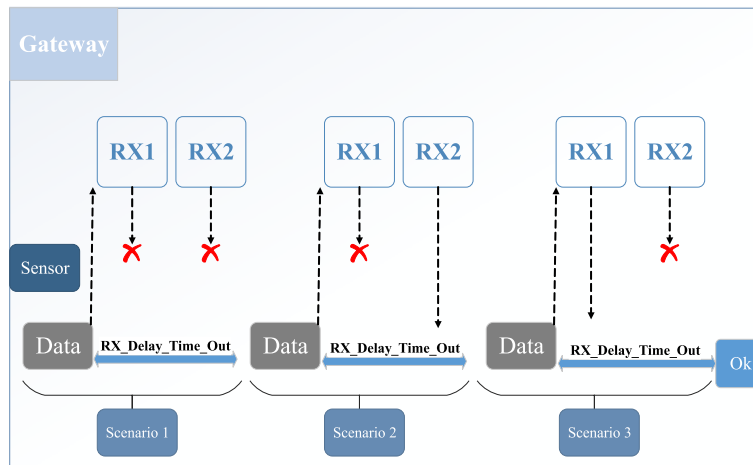


**Fig. 6** Sensor scenarios

MHz. Table 3 illustrates the power and time parameters of the model. These parameters are given in the datasheets of BMA220, STM32L073, and SX1272 [40, 44, 45].

**6.1 Consumed energy: scenario 1**

In this scenario, we suppose that the sensor node has not received RX1 and RX2. The main energy consumers are the micro-controller unit, the sensor unit, and the transceiver unit. Suppose the downlink message is lost for any reason. The LoRa specification recommends sending packets up to 8 times. Figure 7 presents the energy consumption

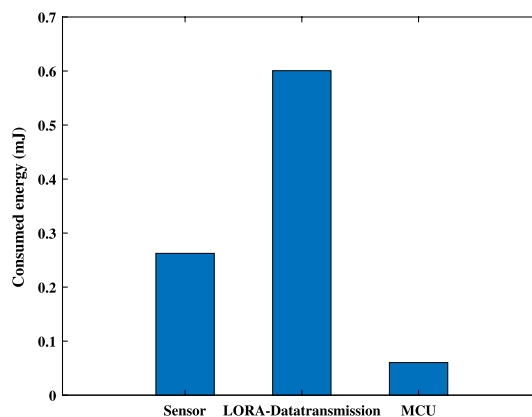


**Fig. 7** Energy consumption of sensor node: scenario 1

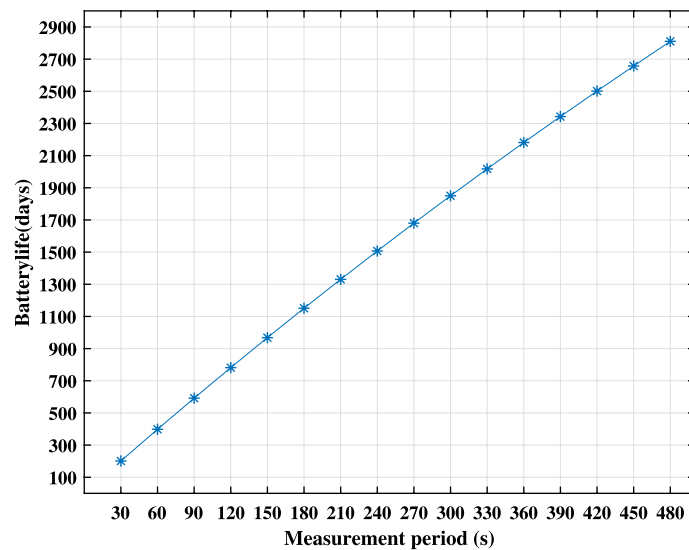


**Fig. 8** Sensor node lifetime: scenario 1

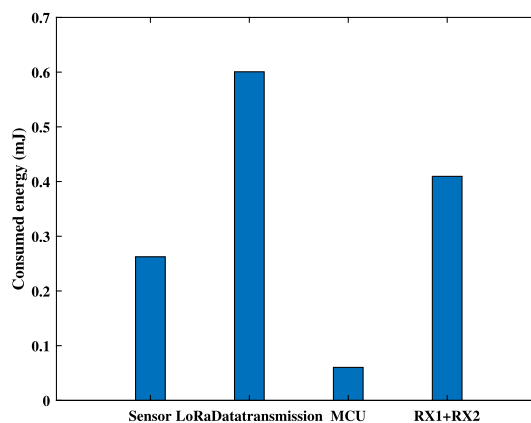


**Fig. 9** Energy consumption of sensor node: scenario 2

amount of the principal communicating sensor. As shown in Fig. 7, MicroMontroller Unit (MCU) consumes energy during all active stages which are denoted by  $E_{MCU}$ , so the major energy consumers can be calculated from Table 3 as follows: the ( $E_{MCU} = 0.0603$  mJ), the sensor unit ( $E_m = 0.2625$  mJ) and the LoRa Data transmission ( $E_{Tr} = 0.6006$  mJ), while other consumed energies, i.e.,  $E_{WU}$ ,  $E_{Proc}$ , and  $E_{WUT}$  are around  $2 \mu J$  each and can be neglected. The sensor node lifetime illustrated in Fig. 8 uses the battery characteristics with a capacity equal 50 mAh, and a supply voltage of 3 V. The sensor node autonomy is about 201 days when the measurement period is equal to 30 s.

**6.2 Consumed energy: scenario 2**

In this scenario, the sensor node transfers data to the gateway and then receives an acknowledgment RX2 without receiving RX1 to verify that the transmission was successful. The energy consumption by the communicating sensor is illustrated in Fig. 9. As shown, the distinction from Scenario 1 is the dissipated energy by the LoRa receiver RX2 ( $E_{R2} = 0.42$  mJ) and the consumed energy by the MCU unit. Figure 10 presents the

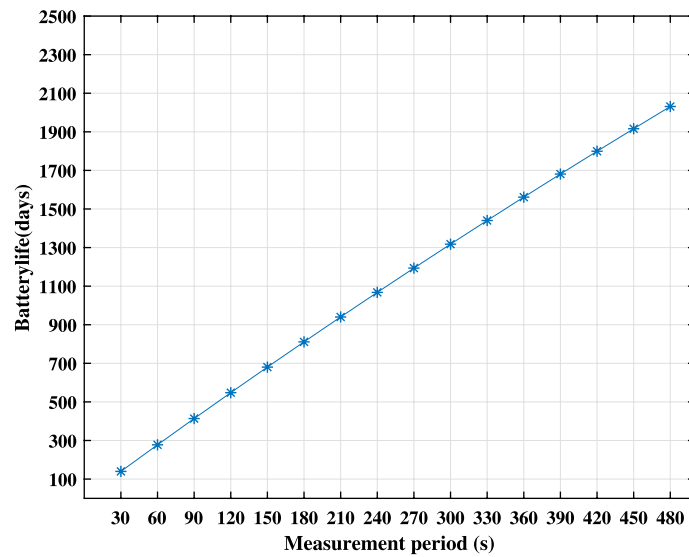


**Fig. 10** Sensor node lifetime: scenario 2

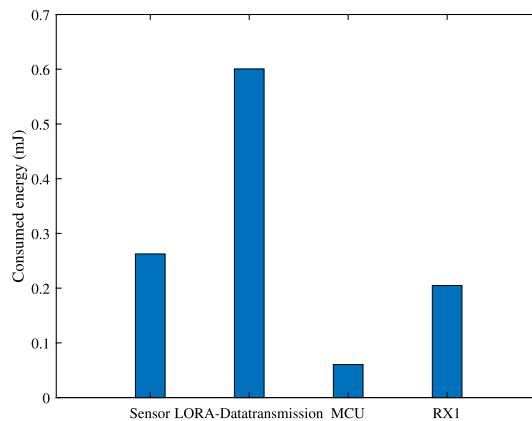


**Fig. 11** Sensor node lifetime: scenario 3

sensor node lifetime using the battery characteristics (capacity equals 50 mAh and supply voltage of 3 V). The sensor node autonomy is about at 139 days when the measurement period is equal to 30 s less than Scenario 1.

### 6.3 Consumed energy: scenario 3

For this scenario, we assume that the sensor node transmits data to the gateway and then receives RX1 acknowledgment excluding the RX2 acknowledgment to verify the transmission success, which means that it will consume more energy than scenario 2. The dissipated energy by the communicating sensor is given in Fig. 11. We note that the consumed energy is half that consumed by the LoRa receiver Rx1 ( $ER = 0.21$  mJ). The sensor node lifetime is illustrated in Fig. 12 using the battery characteristics (capacity equals 50 mAh and a supply voltage of 3 V). The sensor node autonomy is about 164 days when the measurement period is equal to 30 s.

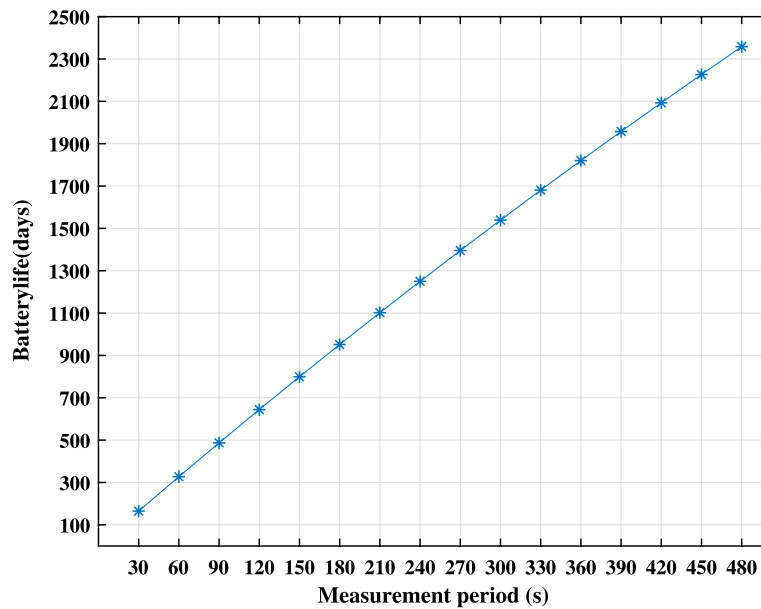


**Fig. 12** Sensor node lifetime: scenario 3

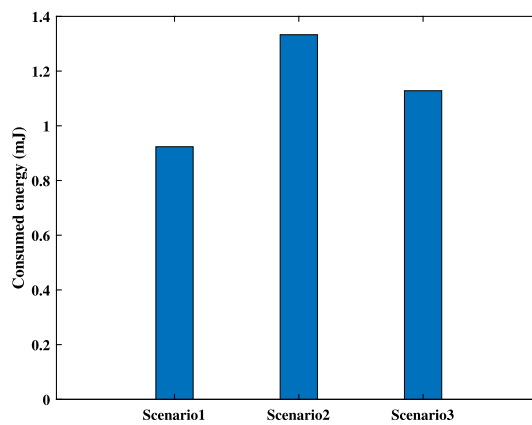


**Fig. 13** Energy consumption for all scenarios

#### 6.4 Comparison between proposed scenarios

A theoretical lifetime of an end-device is computed, employing average energy consumption results acquired for unacknowledged transmission and acknowledged transmission by using equations 16, 17, and 18. Figures 13 and 14 show the results of energy consumption and battery life for these scenarios. The sensor node lifetime in the ideal case (data transmission with reception acknowledgment and without transmission error). It can be clearly seen how each scenario affects the energy consumption battery lifetime and the battery self-discharge considered.

Table 4 illustrates a comparison between the proposed scenarios. As we can notice, the sensor node lifetime in Scenario 1 is higher than in Scenarios 2 and 3. These findings indicate the energy consumption cost of receiving downlink messages from the gateway. Proportionally, SFs have a proportional relationship with average energy consumption

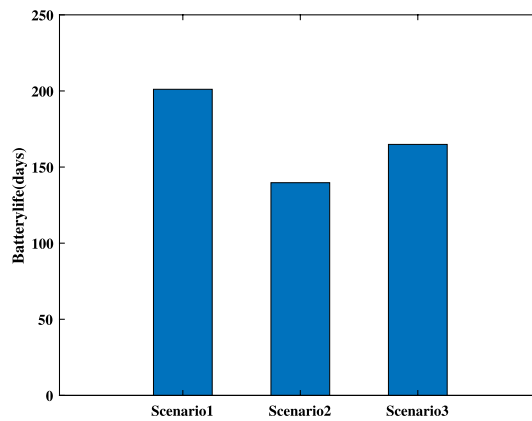


**Fig. 14** Sensor node lifetime for all scenarios

**Table 4** Effect of different scenario about ACK energy consumption

Scenario	Characteristics	Energy consumption (mJ)
Scenario 1	RX1 and RX2 not received	$E_{LRX} = 0$
Scenario 2	RX1 not received; RX2 received	$E_{LRX} = 0.40$
Scenario 3	RX1 received	$E_{LRX} = 0.20$

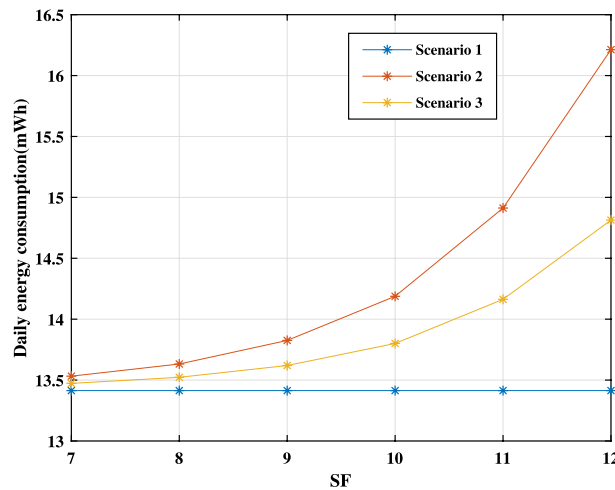


**Fig. 15** Energy consumption of sensor node for all scenarios

as transmit and receive intervals of sensor nodes as a function of Bandwidth illustrated in Fig. 15. However, the daily energy consumption is inversely correlated with each Bandwidth illustrated in Fig. 16 as a function of SF. Furthermore, the time-on-air (ToA) increases with decreasing bit rate as a function of SF. LoRaWAN network capacity can sustain millions of messages. However, the number of packets maintained in any provided deployment relies on the number of gateways that are installed. A single eight-channel gateway can support a few hundred thousand messages throughout 24 h [46].

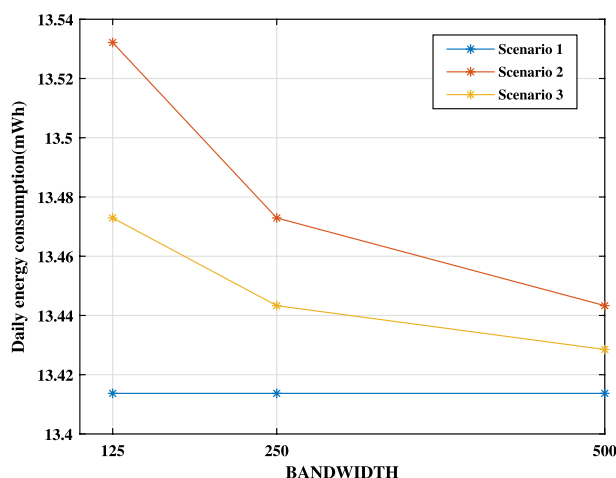
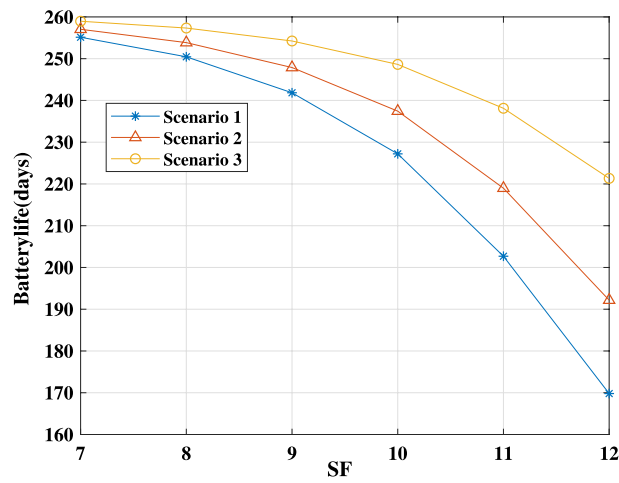


Fig. 16 Sensor node lifetime for all scenarios

### 7 Results and discussion

In this section, we use the models derived in “Methods/experimental” section to evaluate LoRaWAN end-device energy consumption in a different scenario, as well as the battery lifetime. As further validation of the evaluation results, we have performed the power transmission time measurements every 8 min, comprising several message transmissions from the end device, for the same configurations in terms of DR, different values of SF, notification period, and acknowledged or unacknowledged transmission. We have found an almost precise match between the measured energy consumption and the one computed by using the analytical models. Emphasize that this is an expected result since the analytical models have been derived based on simulation results. As shown in Figs. 17 and 18, the evaluation of the battery life when the power transmission is equal to 7 dBm and 17 dBm, respectively, for all scenarios. After employing the proposed model, the simulation results show the different improvements in terms of increasing the battery lifetime and decreasing the energy consumption for each scenario. To be able to evaluate the proposed model under various conditions, Figs. 19 and 20 present the battery Life for Scenario 1 and Scenario 3 when the power transmission takes distinct values. The results show increased energy consumption due to the rise of the power transmission time and SF values. From our obtained results, we can realize that after applying the proposed model, the improvement of increasing battery life reaches almost 259 days when the SF value is 7 for scenario 3. Table 5 describes an evaluation that gives more insights into the improvements applied for each scenario with different values of SF and  $P_{tr}$ .

The results in Figs. 21 and 22 confirmed that the consumed energy increases with the increase of the value of SF, and the power transmission. Assuming that the value of power transmission time increases from 7 dBm and 13 dBm to 17 dBm, and to 20 dBm, respectively, applies to Scenario 1 and Scenario 3. This leads to the efficient use of the proposed model presented in Figs. 23 and 24. This minimizes the consumed energy, as well as the best Scenario, is 3 when the transmission power is 7 dBm and SF is equal to 7, so the consumed energy per day is 13.51 mWh. Table 5 presents a comparison between the proposed scenarios. As we can see, the battery lifetime in Scenarios 2 and 3 is higher



**Fig. 17** Battery life when Ptr = 7 for all scenarios

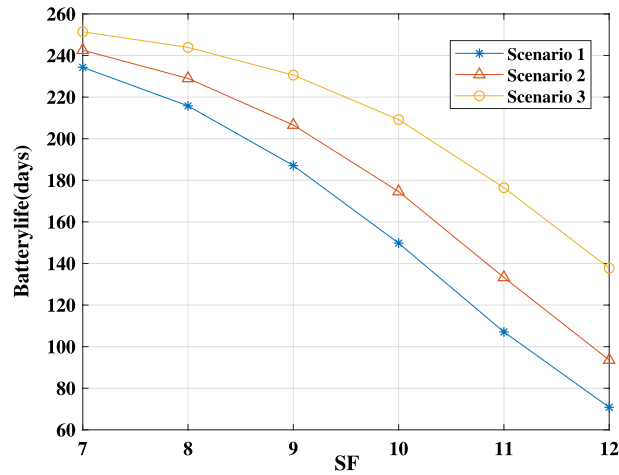


**Fig. 18** Battery life when Ptr = 17 for all scenarios

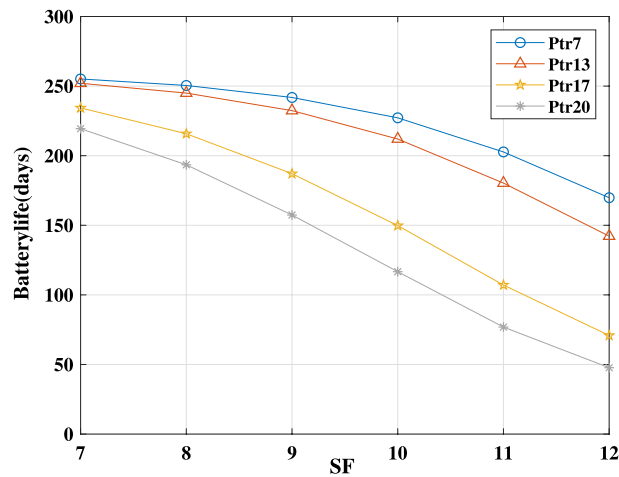


**Fig. 19** Battery life for scenario 1

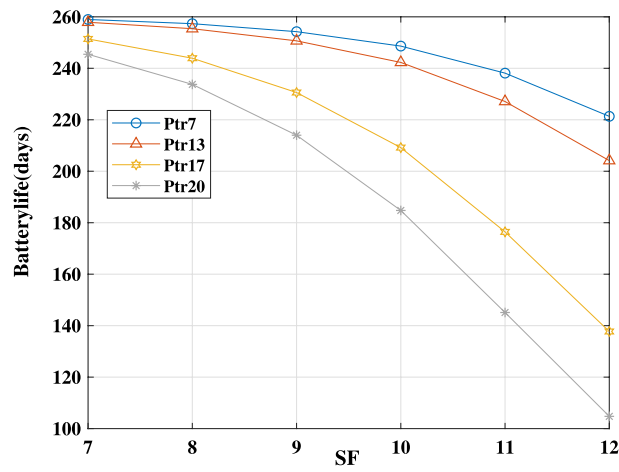


**Fig. 20** Battery life for scenario 3

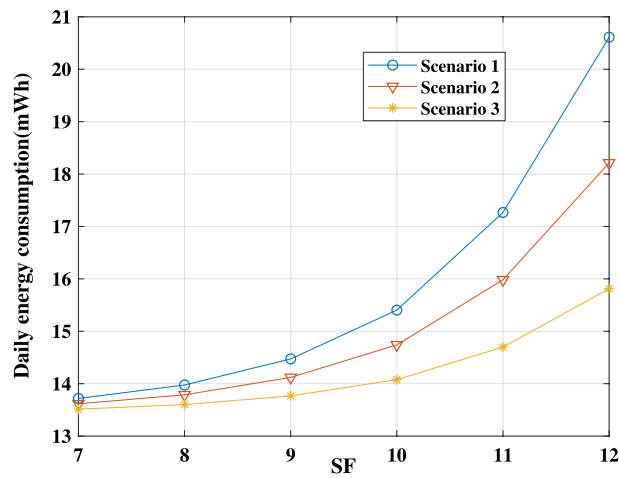


**Fig. 21** Daily energy consumption Pt = 7

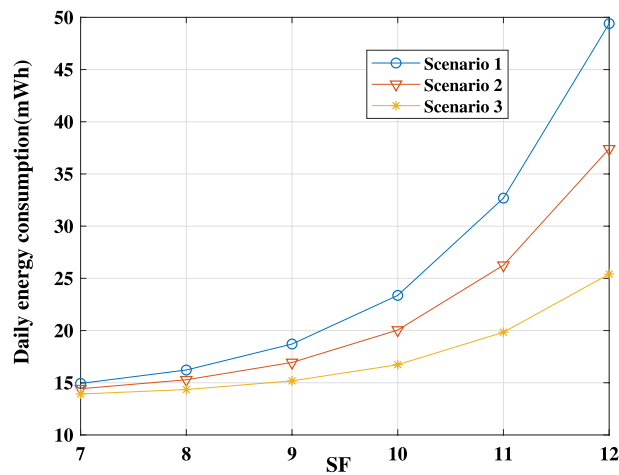


**Fig. 22** Daily energy consumption Pt = 17

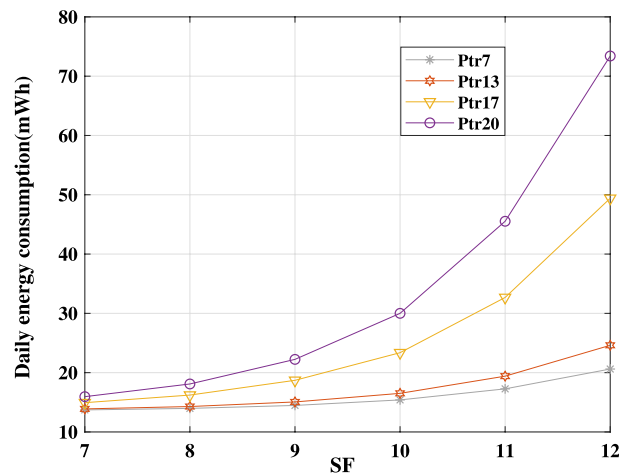


**Fig. 23** Daily energy consumption for scenario 1

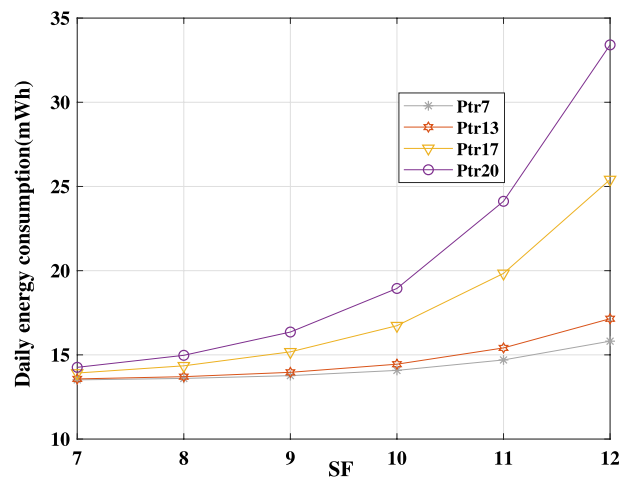


**Fig. 24** Daily energy consumption for scenario 3

than in Scenario 1, because the consumed energy is less when the time of the power transmitted is lower, respectively. These results show the energy consumption cost of receiving downlink messages from the gateway.

To show the effect of different time intervals when we send periodic messages on the daily energy consumption and battery lifetime, we refer to Figs. 25 and 26. We note that the energy consumption of the node depends on how often we are transmitting the message per day (it increases with frequency and SF).

### 8 Conclusion

Communicating over long distances using minimal energy is an intricate task. LPWANs attain this by constructing star topology networks, that permit devices to communicate directly with a gateway without any relaying of messages. By employing slow and straightforward modulation techniques, LPWAN devices operate efficiently to have a high energy per bit and, accordingly, a strong signal. The most standard carrier waves in LPWANs are narrowband waveforms that modulate a limited bandwidth that will

**Table 5** Summary of energy consumption and battery life time

Scenarios	Transmission power (dBm)	SF	Energy consumption per day (mWh)	Battery lifetime (days)
Scenario 1	7	7	13.71	255.1
		8	13.97	250.4
		9	14.47	241.8
		10	15.40	227.2
		11	15.98	202.7
		12	18.21	169.8
	17	7	14.93	234.3
		8	16.22	215.8
		9	18.70	187.0
		10	23.36	149.7
		11	32.28	107.1
		12	49.40	70.8
Scenario 2	7	7	13.61	257.0
		8	13.78	253.8
		9	14.11	247.9
		10	14.74	237.4
		11	15.98	218.9
		12	18.21	192.2
	17	7	14.42	242.6
		8	15.28	228.9
		9	16.94	206.56
		10	20.04	174.6
		11	26.26	133.3
		12	37.40	93.6
Scenario 3	7	7	13.51	258.9
		8	13.60	257.3
		9	13.76	254.2
		10	14.07	248.6
		11	14.69	238.1
		12	15.81	221.3
	17	7	13.92	251.4
		8	14.34	243.9
		9	15.18	230.6
		10	16.73	209.2
		11	19.84	176.4
		12	25.41	137.7

emerge as a peak and Spread waveforms to distribute the signal out and later retrieve it utilizing post-processing techniques. A common factor for them all is that they have a low protocol overhead.

Energy consumption is one of the main objectives in the procedure of designing and developing a sensor network. In this research, we consider the energy consumption of the Class A model that has been presented for dense LoRaWAN network viewing the information transmitted at periodic intervals between the end nodes and gateways in confirmed and unconfirmed transmission. We presented thorough numerical results of the average energy consumption in acknowledged and unacknowledged transmission

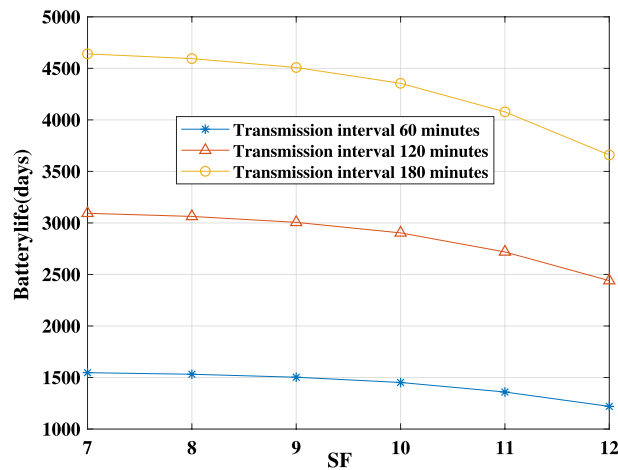


Fig. 25 Battery life time for different time

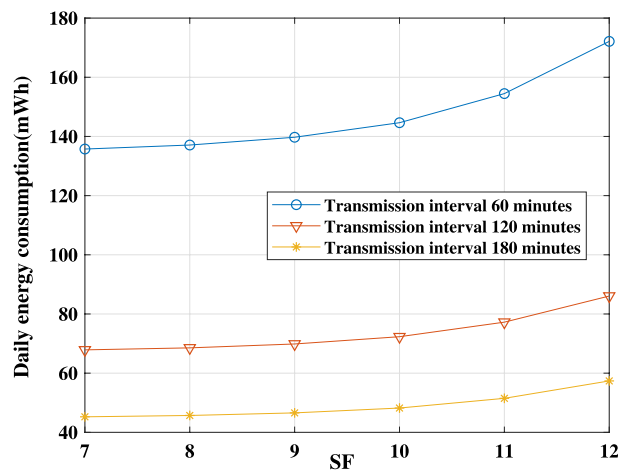


Fig. 26 Daily energy consumption for different time

by proposing different LoRaWAN scenarios. To evaluate the energy consumption of the sensor node, we concluded that receiving a transmission acknowledgment consumes an energy amount which reduces the lifetime of a sensor node. Moreover, Optimizing different LoRa/LoRaWAN parameters such as spreading factor, coding rate, payload size, and bandwidth is essential to decrease the energy consumption of the sensor node. The proposed sensor node operating on a 50 mAh battery that transmits one message to the gateway every 30 s with the higher spreading factor (SF) can have a theoretical lifetime of up to 2.78 years as compared to 4.4 years for lower SF.

Finally, the energy efficiency of the LoRaWAN network is studied concerning the specific average number of nodes. Furthermore, we illustrated the superiority of lower over higher spreading factor in terms of energy efficiency over a circular coverage area. The optimal trade-off between power consumption and other device parameters relies on the specific application and use case. The results of this research paper could be used to understand the relationship between device variables and power consumption. In future work, the energy model can be further investigated using the choice of

the antenna and how it can affect the range and reliability. Also, the investigation of the co-existence between narrowband and spread wave technologies is an important topic. Additional elements could be added to the proposed model, such as processing power based on the operating frequency to maximize the sensor node lifetime.

#### Abbreviations

IoT	Internet of Things
LPWAN	Low-power wide area network
RFID	Radio-frequency identification
QR	Quick response
MTC	Machine-type communications
CSS	Chirp spreading spectrum
CR	Coding rate
BW	Bandwidth
NS	The network server
SF	Spreading factor
ToA	The time-on-air
CF	Carrier frequency
PER	Packet error rate
$N_{\text{pload}}$	The number of payload symbols
PL	Number of payload bytes
CRC	Cyclic redundancy check
$n_{\text{preamble}}$	The number of preamble symbols
$t_{\text{packet}}$	The packet duration
$P_{\text{TX}}$	The transmission power consumption
$E_{\text{packet}}$	The energy consumption per transmission
$N_{\text{msg}}$	The number of data transfers per day
$T_C$	The current sending cycle
ADC	Analog to digital converter
CPU	Central processing unit
$E_{\text{TOTAL}}$	The total consumed energy
$E_{\text{Active}}$	The energy consumed when the system is active
$E_{\text{Sleep}}$	The energy consumed when the system is in sleep mode
$P_{\text{Sleep}}$	The power consumption in sleep mode
$t_{\text{Sleep}}$	The duration in sleep mode
$LT$	The lifetime of the devices
$E_{\text{Bat}}$	The battery capacity
$E_{\text{day}}$	The energy consumption per day
$n_{\text{msg}}$	The number of transactions,
$C_{\text{Battery}}$	The battery capacity
$D_{\text{BL}}$	The battery life

#### Acknowledgments

This research is supported by Tempus Public Foundation, Stipendium Hungaricum Scholarship Programme and High Speed Networks Lab, Department of Telecommunications and Media Informatics, Budapest University of Technology and Economics.

#### Author contributions

HR as the principal investigator takes the primary responsibility for this research and analyzed the results. All authors read and approved the final manuscript. TB conceived of the study, and participated in its design and coordination and helped to draft the manuscript.

#### Funding

This work was supported by the Ericsson - BME 5 G joint research and cooperation project, partly funded by the National Research, Development and Innovation Office, Hungary with project number 2018-1.3.1-VKE-2018-00005.

#### Availability of data and materials

The data used to support the findings of this study are available from the corresponding author upon request.

#### Declarations

##### Competing interests

The authors declare that they have no competing interests.

Received: 30 August 2022 Accepted: 1 November 2023

Published online: 13 December 2023

## References

1. S. Chen, H. Xu, D. Liu, B. Hu, H. Wang, A vision of IoT: applications, challenges, and opportunities with China perspective. *IEEE Internet Things J.* **1**, 349–359 (2014)
2. A. Triantafyllou, P. Sarigiannidis, T.D. Lagkas, Network protocols, schemes, and mechanisms for internet of things (IoT): features, open challenges, and trends. *Wirel. Commun. Mob. Comput.* **2018** (2018)
3. R.M. Sandoval, A.-J. Garcia-Sanchez, J. Garcia-Haro, Performance optimization of LoRa nodes for the future smart city/industry. *EURASIP J. Wirel. Commun. Netw.* **2019**, 1–13 (2019)
4. M.R. Palattella, M. Dohler, A. Grieco, G. Rizzo, J. Torsner, T. Engel, L. Ladid, Internet of Things in the 5G era: enablers, architecture, and business models. *IEEE J. Sel. Areas Commun.* **34**(3), 510–527 (2016)
5. R. Oliveira, L. Guardalben, S. Sargento, Long range communications in urban and rural environments, in *Proceedings of the IEEE Symposium on Computers and Communications Conference (ISCC)*, Heraklion, Greece, 3–6 July (2017)
6. M. Elodie, M. Mickael, G. Roberto, D. Andrzej, Comparison of the device lifetime in wireless networks for the Internet of Things. *IEEE Access* **5**, 7097–7113 (2017)
7. R.S. Sinha, Y. Wei, S.-H. Hwang, A survey on LPWA technology: LoRa and NB-IoT. *ICT Express* **3**(1), 14–21 (2017)
8. U. Raza, P. Kulkarni, M. Sooriyabandara, Low power wide area networks: an overview. *IEEE Commun. Surv. Tutor.* **19**(2), 855–873 (2017)
9. A. Augustin, J. Yi, T. Clausen, W.M.A. Townsley, Study of LoRa: long range and low power networks for the internet of things. *Sensors* **16**(9), 1466 (2016)
10. J. Haxhibeqiri, E. De Poorter, I. Moerman, J. Hoebeke, A survey of LoRaWAN for IoT: from technology to application. *Sensors* **18**(11), 3995 (2018)
11. Libelium. Waspromote-LoRa-868MHz-915MHz-SX1272 Networking Guide, v7.0; Libelium: Zaragoza, Spain, (2017)
12. ST Microelectronics, *STM32 Nucleo Pack for LoRa Technology (P-NUCLEO-LRWAN1)*, DocID029505 Rev. 2 (ST Microelectronics, Geneva, 2016)
13. NetBlocks Embedded Networking. XRange SX1272 LoRa RF module. <http://www.netblocks.eu/>. Accessed 11 Aug 2020
14. M. Asad Ullah, J. Iqbal, A. Hoeller, R.D. Souza, H. Alves, K-means spreading factor allocation for large-scale LoRa networks. *Sensors* **19**(21), 472 (2019)
15. Martin, B., Roedig, U., LoRa transmission parameter selection, in *2017 13th International Conference on Distributed Computing in Sensor Systems (DCOSS)* (IEEE, 2017), pp. 27–34
16. K.E. Nolan, W. Guibene, Y.K. Mark, An evaluation of low power wide area network technologies for the Internet of Things, in *2016 International Wireless Communications and Mobile Computing Conference (IWCMC)* (IEEE, 2016), pp. 439–444
17. J. Petäjärvi, K. Mikhaylov, R. Yasmin, M. Hämäläinen, J. Linatti, Evaluation of LoRa LPWAN technology for indoor remote health and wellbeing monitoring. *Int. J. Wirel. Inf. Netw.* **24**(2), 153–165 (2017)
18. O. Iova, A.L. Murphy, L. Ghiro, D. Molteni, F. Ossi, F. Cagnacci, LoRa from the city to the mountains: exploration of hardware and environmental factors, in *Proceedings of the 2nd International Workshop on New Wireless Communication Paradigms for the Internet of Things (MadCom)*, Uppsala, Sweden (2017), pp. 20–22
19. P.J. Marcellis, S. Vijay, R. Rao, V. Prasad, DaRe: data recovery through application layer coding for LoRaWAN, in *2017 IEEE/ACM Second International Conference on Internet-of-Things Design and Implementation (IoTDI)* (IEEE, 2017), pp. 97–108
20. M. Cattani, C.A. Boano, K. Römer, An experimental evaluation of the reliability of LoRa long-range low-power wireless communication. *J. Sens. Actuator Netw.* **6**(2), 7 (2017)
21. B. Kim, K. Hwang, Cooperative downlink listening for low-power long-range wide-area network. *Sustainability* **9**(4), 627 (2017)
22. D. Sartori, D. Brunelli, A smart sensor for precision agriculture powered by microbial fuel cells, in *2016 IEEE sensors applications symposium (SAS)* (IEEE, 2016), pp. 1–6
23. M. Srbínovska, V. Dimcev, C. Gavrovski, Energy consumption estimation of wireless sensor networks in greenhouse crop production, in *IEEE EUROCON 2017-17th International Conference on Smart Technologies* (IEEE, 2017), pp. 870–875
24. S. Cheong, Phui, J. Bergs, C. Hawinkel, J. Famaey, Comparison of LoRaWAN classes and their power consumption, in *2017 IEEE Symposium on Communications and Vehicular Technology (SCVT)* (IEEE, 2017), pp. 1–6
25. O. Georgiou, U. Raza, Low power wide area network analysis: Can LoRa scale? *IEEE Wirel. Commun. Lett.* **6**(2), 162–165 (2017)
26. P. Neumann, J. Montavont, T. Noël, Indoor deployment of low-power wide-area networks (LPWAN): a LoRaWAN case study, in *2016 IEEE 12th International Conference on Wireless and Mobile Computing, Networking and Communications (WiMob)* (IEEE, 2016), pp. 1–8
27. K. Mikhaylov, J. Petäjärvi, Design and implementation of the plug and play enabled flexible modular wireless sensor and actuator network platform. *Asian J. Control* **19**(4), 1392–1412 (2017)
28. J. Gaelens, P. Van Torre, J. Verhaever, H. Rogier, LoRa mobile-to-base-station channel characterization in the Antarctic. *Sensors* **17**(8), 1903 (2017)
29. L. Casals, B. Mir, R. Vidal, C. Gomez, Modeling the energy performance of LoRaWAN. *Sensors* **17**(10), 2364 (2017)
30. Alliance LoRa. LoRa Alliance (2019). <https://lora-alliance.org>. Visited 20 Aug 2020
31. K.-H. Phung, H. Tran, Q. Nguyen, T.T. Huong, T.-L. Nguyen, Analysis and assessment of LoRaWAN, in *2018 2nd International Conference on Recent Advances in Signal Processing, Telecommunications and Computing (SigTelCom)* (IEEE, 2018), pp. 241–246
32. J. de Carvalho Silva, J.J.P.C. Rodrigues, A.M. Alberti, P. Solic, A.L.L. Aquino, LoRaWAN-A low power WAN protocol for Internet of Things: a review and opportunities, in *2017 2nd International Multidisciplinary Conference on Computer and Energy Science (SpliTech)* (IEEE, 2017), pp. 1–6
33. A. Pötsch, F. Haslhofer, Practical limitations for deployment of LoRa gateways, in *2017 IEEE International Workshop on Measurement and Networking (M and N)* (IEEE, 2017), pp. 1–6

34. F. Cuomo, M. Campo, A. Caponi, G. Bianchi, G. Rossini, P. Pisani, EXPLoRa: extending the performance of LoRa by suitable spreading factor allocations, in *2017 IEEE 13th International Conference on Wireless and Mobile Computing, Networking and Communications (WiMob)* (IEEE, 2017), pp. 1–8
35. J. Burns, S. Kirtay, P. Marks, Future use of licence exempt radio spectrum. Plum Consulting, London, UK, Technical report (2015)
36. M. Lauridsen, B. Vejlggaard, I.Z. Kovács, H. Nguyen, P. Mogensen, Interference measurements in the European 868 MHz ISM band with focus on LoRa and SigFox, in *2017 IEEE Wireless Communications and Networking Conference (WCNC)* (IEEE, 2017), pp. 1–6
37. F. Guillaume, E. Simon, An introduction to Sigfox and LoRa PHY and MAC layers (2018)
38. K. Matt, Reversing LoRa: exploring next-generation wireless (2016)
39. E. Dubrova, *Fault-Tolerant Design* (Springer, New York, 2013)
40. Semtech Corporation. SX1272/3/6/7/8: LoRa Modem. Designer's Guide. AN1200.13 (Semtech Corporation, Camarillo, CA, USA, 2013). <https://rb.gy/hi0bez>. Accessed 26 Sept 2020
41. T. Bouguera, J.-F. Diouris, J.-J. Chaillout, R. Jaouadi, G. Andrieux, Energy consumption model for sensor nodes based on LoRa and LoRaWAN. *Sensors* **18**(7), 2104 (2018)
42. T. Guillaume, A. Llaría, R. Briand, System level dimensioning of low power biomedical body sensor networks, in *2014 IEEE Faible Tension Faible Consommation* (IEEE, 2014), pp. 1–4
43. C. Delgado, J. María Sanz, C. Blondia, J. Famaey, Battery-less LoRaWAN communications using energy harvesting: modeling and characterization. *IEEE Internet Things J.* **8**, 2694–2711 (2020)
44. BMA220 Digital, Triaxial Acceleration Sensor Data Sheet. <http://image.dfsrobot.com/image/data/SEN0168/BMA220%20datasheet.pdf>. Accessed 26 Sept 2020
45. STM32L073x8 STM32L073xB STM32L073xZ Data Sheet; ST Microelectronics Document. <https://www.st.com/resource/en/datasheet/stm32l073v8.pdf>. Accessed 26 Sept 2020
46. H. Rajab, T. Cinkler, T. Bouguera, IoT scheduling for higher throughput and lower transmission power. *Wirel. Netw.* **27**, 1–14 (2020)

### Publisher's Note

Springer Nature remains neutral with regard to jurisdictional claims in published maps and institutional affiliations.

**Husam Rajab** received a B.Sc. degree in Computer and Communication Engineering at Al-Azhar University, Gaza, Pales-tine, in 2013. He received and M.Sc. degree in Electrical and Communication Engineering at Beijing University of Posts and Telecommunication in 2017. He received his PhD in June 2023, studied at the Department of Telecommunications and Media Informatics at Budapest University of Technology and Economics, Hungary. His main research interests are the Internet of Things, Radio Resource Management and QoS control for next-generation mobile and wireless networks, Machine Learning, cognitive radio, spectrum sensing.

**Husam Al-Amaireh** received his Ph.D. degree in Electric Engineering from the Budapest University of Technology and Economics (BME) in 2021. He was a member of BME MATLAB Laboratory. His research interest are digital signal processing, FBMC, massive MIMO and IoT.

**Taufik Bouguera** has received the B.Sc. degree in telecommunication engineering in 2015 and the M.Sc. degree in telecommunication systems from the National Engineering School of Tunis (ENIT), Tunisia. He received a Ph.D. from the University of Nantes in 2019, and his thesis project in the realization of an energy-autonomous communication sensor for IoT applications. He is currently an IoT project manager in Astek Group Paris. His research interests include the new low power wide area technologies and energy optimization and mobile networks.

**Tibor Cinkler** has received M.Sc. (1994) and Ph.D. (1999) degrees from the Budapest University of Technology and Economics(BME), Hungary, where he is currently a full professor at the Department of Telecommunications and Media Informatics (TMIT). He habilitated in 2013 and received the D.Sc. degree from the Hungarian Academy of Sciences the same year. He has been visiting professor at the Department of Computer Communications of the Gdansk University of Technology, Poland in the academic year of 2018/2019. His research interests focus on the optimization of routing, traffic engineering, design, configuration, dimensioning and resilience of IP, Ethernet, MPLS, OTN, 4G/5G and particularly of heterogeneous GMPLS-controlled WDM-based multi-layer networks. He is author of over 300 refereed scientific publications including four patents, with over 2200 citations.